Ultrathin fluorinated silicon nitride gate dielectric films formed by remote plasma enhanced chemical vapor deposition employing NH_3 and SiF_4

Hiroyuki Ohta, Masaru Hori,[a] and Toshio Goto
Department of Quantum Engineering, Graduate School of Engineering, Nagoya University, Furo-cho, Chikusa-ku, Nagoya 464-8603, Japan

(Received 18 December 2000; accepted for publication 1 May 2001)

Ultrathin fluorinated silicon nitride (SiN_x) films of 4 nm in thickness were formed on a Si substrate at 350 °C in the downflow of electron cyclotron resonance plasma-enhanced chemical vapor deposition employing ammonia and tetrafluorosilane (NH_3/SiF_4) gases. Ultrathin fluorinated SiN_x film was evaluated for use as a gate dielectric film. The observed properties indicated an extremely low leakage current, one order of magnitude lower than thermal SiO_2 of identical equivalent oxide thickness, as well as an excellent hysteresis loop (20 mV) and interface trap density ($D_{it}=4\times10^{11}\,cm^{-2}$) in the capacitance–voltage characteristics. The film structures and the surface reactions for the fluorinated SiN_x film formation were examined via *in situ* x-ray photoelectron spectroscopy. *in situ* Fourier-transform infrared reflection absorption spectroscopy, *in situ* atomic force microscopy, and thermal desorption mass spectroscopy. The control of the fluorine concentration in the SiN_x films was found to be a key factor in the formation of fluorinated SiN_x films of high quality at low temperatures. Fluorinated SiN_x is the effective material for application in ultrathin gate dielectric film in ultralarge-scale integrated circuits. © *2001 American Institute of Physics.* [DOI: 10.1063/1.1381556]

I. INTRODUCTION

As device dimensions shrink to below 0.1 μm in ultralarge-scale integrated circuits (ULSIs), the thickness of the gate dielectric film (SiO_2) in field effect transistors will fall to $\leq$2 nm range, which leads to leakage due to a tunneling current. In principle, the SiO_2 film is replaced by a dielectric film of a higher dielectric constant, since the physical thickness can be increased to be above 3 nm according to the scaling limit.[1] Silicon nitride (SiN_x) film has attracted as much attention as a possible scaled gate dielectric film in next-generation ULSIs. Since the dielectric constant of SiN_x film ($\epsilon=7.5$) is higher than that of SiO_2 ($\epsilon=3.9$), the thickness can be increased. Furthermore, SiN_x film is compatible with the conventional process involved in ULSI formation and has a high diffusion barrier for boron penetration. As one approach, future high-speed ($\geq$1 GHz) ULSIs will require the introduction of metal substrate silicon-on-insulator (SOI) devices.[2] In order to fabricate metal substrate SOI devices, all of the manufacturing processes have to be performed at a temperature below 550 °C in order to avoid unexpected reactions between Si and metals. Moreover, in order to realize ultrahigh integration devices with precise doping profile control, all of the manufacturing processes must be performed at temperatures below 550 °C so as to prevent rediffusion of impurities injected in the substrate. In order to establish complete low temperature processing below 550 °C, lowering the process temperature of integration with the SiN_x film formation is critical. Chemical vapor deposition (CVD) techniques such as plasma-enhanced CVD (PECVD) and remote PECVD, and plasma-nitridation of Si substrate in N_2 atmosphere present the advantage of lowering the substrate temperature.[3–5] Unfortunately, although the low-temperature processes generally meet the low-temperature and low-thermal budget constraints for ULSI applications, the electrical performance of SiN_x films formed by PECVD are marginal, primarily due to the high current leakage at low electrical fields, and high densities of traps at their interfaces with Si.[6] In our previous works, it was reported that ultrathin SiN_x films of good quality were formed while controlling the radicals and ions in electron cyclotron resonance (ECR) plasma employing nitrogen and silane (N_2/SiH_4)[7] and ammonia and silane (NH_3/SiH_4).[8] As a result, NH_4^+ charged species were found to be important in the formation of the Si–N network for the forming of SiN_x films of high quality in PECVD employing NH_3/SiH_4. However, large concentrations of hydrogen are contained in ultrathin SiN_x film formed employing NH_3/SiH_4 and these hydrogen bonds may act as deep traps in the film. Therefore, in order to improve metal–nitride–semiconductor (MNS) characteristics in future devices, the amount of hydrogen incorporated should be reduced and/or the formation of stable hydrogen bonds in the films are desired. However, no report has been presented of the formation of ultrathin SiN_x film in order to control the hydrogen densities and hydrogen bonds at low temperature.

In the present study, we synthesize ultrathin fluorinated SiN_x films of 4 nm in thickness having a low leakage current, an excellent hysteresis loop, and a low interface trap density. The ultrathin SiN_x films were formed by remote ECR–PECVD employing ammonia and tetrafluorosilane (NH_3/SiF_4) gases at 350 °C. The effects of fluorine atoms on

[a]Electronic mail: hori@nuee.nagoya-u.ac.jp

 © 2001 American Institute of Physics

Downloaded 19 Oct 2006 to 133.6.32.11. Redistribution subject to AIP license or copyright, see http://jap.aip.org/jap/copyright.jsp

the ultrathin film property were clarified based on *in situ* x-ray photoelectron spectroscopy (XPS), *in situ* Fourier-transform infrared reflection absorption spectroscopy (FTIR–RAS), FTIR, *in situ* atomic force microscopy (AFM), and thermal desorption spectroscopy (TDS) observations.

II. EXPERIMENT

The typical ECR–PECVD system with a divergence magnetic field was used in the present study, the details of which have been presented in a previous article.[9] In the following section, the CVD system is described briefly. The ECR chamber has an inner diameter of approximately 150 mm and a height of 160 mm. The ECR chamber is mounted on a deposition chamber. Plasma generated by microwave excitation at 2.45 GHz is fed into an 875 G magnetic field that is generated by the magnets surrounding the chamber. The plasma stream is extracted from the ECR chamber into the deposition chamber by a divergent magnetic field. The chamber is pumped by an 1130 L/s turbomolecular pump to achieve a base pressure of 1×10^{-5} Pa. The properties of the plasma were evaluated employing the N_2 gas using single Langmuir probe to be as follows: electron temperatures; below 4 eV, plasma densities; approximately $3\times10^{9}\ \mathrm{cm}^{-3}$, and sheath voltage; approximately 17 V in the downstream plasma region. The N_2 plasma condition was as follows: total pressure, 0.5 Pa; N_2 gas flow rate, 100 sccm; microwave power; 300 W; substrate bias; floating, and substrate temperature, 350 °C.

The SiN_x films were formed by ECR–PECVD employing ammonia and tetrafluorosilane (NH_3/SiF_4) gases. NH_3 gas was fed into the ECR chamber through a shower nozzle near the quartz window. SiF_4 gas was introduced into the deposition chamber near the substrate. In this system, the process chamber was equipped with *in situ* FTIR–RAS. An IR beam was introduced through a polarizer and a KBr window into the process chamber at an incident angle of 80°. The beam was reflected at the substrate and was detected by a mercury–cadmium–telluride detector. The optical path was purged by the dry air in order to avoid the perturbation of water vapor. IR spectra were measured by a Fourier-transformed IR spectrometer (JIR-7000 of JEOL Co.). The wave number resolution of FTIR–RAS was 4 cm^{-1}. A two-layered substrate consisting of aluminum (Al) (600 nm thickness) sputtered onto an n-type (100) silicon substrate in a vacuum was used for FTIR–RAS. The dimensions of the substrate are 4 cm×4 cm. The SiN_x film was deposited on the two-layered substrate. FTIR–RAS has been applied previously in *in situ* observation of the growth process of SiN_x films under ECR PECVD conditions.

In addition, the XPS system (Escalab 220i-XL of FISONS Co.) and the AFM system (UHV–AFM of OMICRON Co.) were connected to the ECR chamber through a transfer chamber in a vacuum. In the XPS system, Mg $K\alpha$ radiation ($h\nu=1253.6$ eV) which allows an overall resolution of 0.7 eV was used as an x-ray source. The SiN_x films formed by ECR–PECVD were transferred to the XPS and AFM chamber without atmospheric exposure. Therefore, the *in situ* FTIR–RAS, *in situ* XPS, and *in situ* AFM analyses enabled the chemical structure of the SiN_x films to be investigated immediately, without exposing the films to the atmosphere following deposition.

SiN_x films were formed on n-type (100) silicon substrates. Silicon substrates were cleaned using HF ($HF:H_2O=1:10$) solution at room temperature before deposition. The physical thickness of the film was measured by *in situ* XPS using the ratio of the bulk Si $2p$ to the chemically shifted Si $2p$, as determined by ellipsometry. The film deposition was performed under the following conditions: total pressure, 0.5 Pa; microwave power, 300 W; substrate bias, floating, and substrate temperature, 350 °C. The mixture ratio of (NH_3/SiH_4 or NH_3/SiF_4) gases was varied from 1.25 to 16.7.

The electrical properties of the SiN_x films were evaluated using Al/SiN_x/Si (n-type) diode structures of Al electrode area 3.98 mm^2 that were prepared especially for the present study. For these samples, no postmetal annealing treatments were performed. The leakage current density–voltage ($J-V$) characteristics were measured by using a semiconductor parameter analyzer (Hewlett-Packard: 4156B). The capacitance–voltage ($C-V$) characteristics were measured using with a commercial measurement system (SSM 5100 system), in which, rather than depositing a gate electrode, $C-V$ measurements were performed using a mercury (Hg) electrode placed above the sample. The area of the Hg electrode was controlled by N_2 gas pressure in the capillary.

III. RESULTS AND DISCUSSION

A. Growth and structure characterization

The SiN_x film was formed employing NH_3/SiH_4 gases and the fluorinated SiN_x film was formed employing NH_3/SiF_4 gases. Figure 1(a) shows FTIR RAS spectra of the ultrathin SiN_x and fluorinated SiN_x film. In the case of the SiN_x films, a frequency component at 1106 cm^{-1} was observed, which consists of a superposition of Si–N and N–H bending mode components. Whereas in the case of the fluorinated SiN_x films, a frequency component at 1087 cm^{-1} was observed, which is attributed to a superposition of Si–N, Si–F stretching mode, and N–H bending mode components. The frequency component (1087 cm^{-1}) of the fluorinated SiN_x films was lower than that (1106 cm^{-1}) of the SiN_x films.[10] This frequency component shift between the SiN_x film and the fluorinated SiN_x film is probably due to the amount of N–H bonds in these films. Figure 1(b) shows the FTIR RAS results for the normalized absorption intensity of Si–N bonds using the fluorine concentration determined by *in situ* XPS, as a function of SiF_4 flow rate. The conditions of NH_3/SiH_4 PECVD were optimized so as to obtain the film composition of near stoichiometry (1.33) which was confirmed by examining the ratio of the N $1s$ peak to the chemically shifted Si $2p$ peak of *in situ* XPS. The mixture ratio of NH_3/SiH_4 was 16.7 ($NH_3/SiH_4=50/3$). By increasing the SiF_4 flow rate, the normalized absorption intensity of Si–N bonds remained unchanged up to SiF_4 gas flow rates of 20 sccm and decreased at flow rates above 20 sccm. The fluorine concentration increased up to flow rates of 20 sccm and

Downloaded 19 Oct 2006 to 133.6.32.11. Redistribution subject to AIP license or copyright, see http://jap.aip.org/jap/copyright.jsp

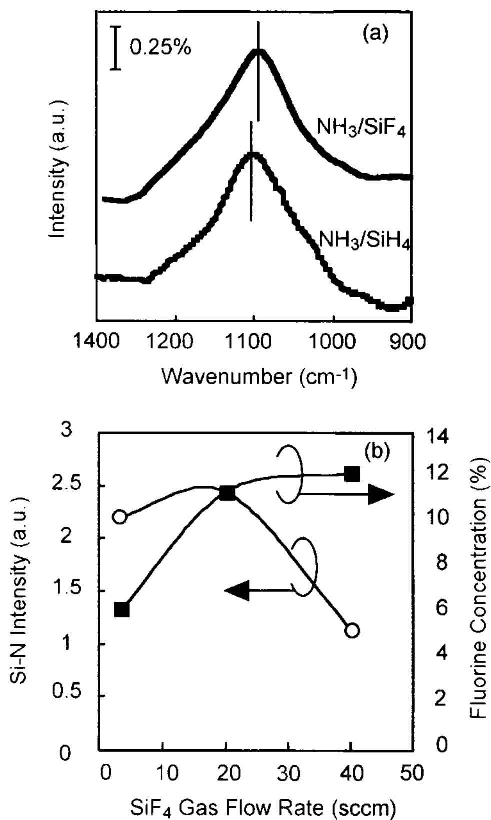

FIG. 1. (a) *In situ* FTIR RAS spectra of ultrathin SiN_x and fluorinated SiN_x films, (b) *in situ* FTIR RAS results of normalized absorption intensity of Si–N_x bonds and fluorine concentration, as a function of SiF_4 flow rate.

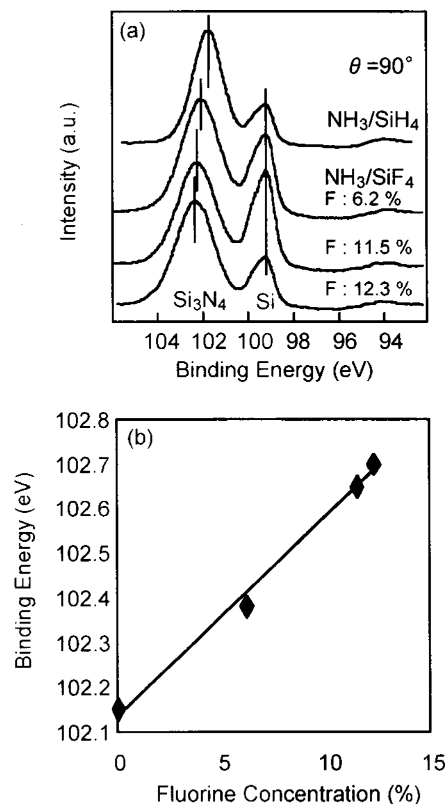

FIG. 3. (a) *In situ* XPS spectra of Si $2p$ and (b) binding energy (relative to E_F) of Si $2p$ core levels of SiN_x films as a function of fluorine concentration.

had a tendency to saturate at flow rates above 20 sccm. These results suggest that fluorines produced from the dissociation of SiF_4 contribute to etching of SiN_x films at high SiF_4 flow rates above 20 sccm.

Based on these results, we optimized the deposition condition of fluorinated SiN_x film in NH_3/SiF_4 PECVD as follows: total pressure, 0.5 Pa; gas flow rate, NH_3/SiF_4=50/20 sccm; microwave power, 300 W; substrate bias, floating, and substrate temperature, 350 °C.

XPS survey spectra of SiN_x film and fluorinated SiN_x film grown at 350 °C are shown in Fig. 2. The Si $2p$, Si $2s$, N $1s$, F $1s$ signals and only a small amount of O $1s$ peak

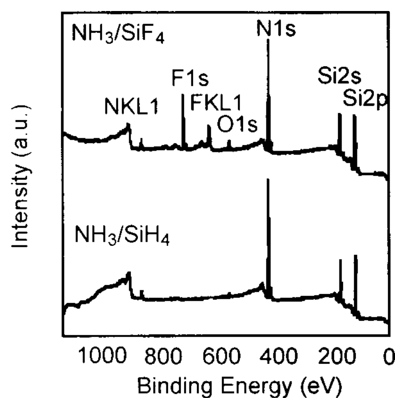

FIG. 2. *In situ* XPS survey spectra of SiN_x film formed employing NH_3/SiH_4 and fluorinated SiN_x film formed employing NH_3/SiF_4.

(~2 at.%) were observed, and the existence of fluorine bonds was confirmed in the fluorinated SiN_x film. The oxygen signal is not attributed to the film, but rather is attributed to the oxygen absorbed onto the silicon surface before deposition because XPS was carried out by *in situ* observation and oxygen peaks were not observed for relatively thick films (above 20 nm). Therefore, the effect of oxygens on the film properties can be neglected in the present study. In addition, film surface roughness was observed using *in situ* AFM. The surface roughness was smooth (rms=1.3 nm) and no remarkable difference was observed between the surface of conventional SiN_x and fluorinated SiN_x films.[7]

The Si $2p$ spectra of conventional SiN_x and fluorinated SiN_x films of various fluorine concentrations are shown in Fig. 3(a). The peak corresponding to Si–N_x bonds is observed at approximately 102 eV. The peak component of the fluorinated SiN_x film consists of a superposition of Si–N_x and Si–F_x bonds. The peak shift of the conventional SiN_x film was the lowest (102.15 eV). Binding energies relative to the Fermi level E_F of the Si $2p$ core levels are plotted in Fig. 3(b) as a function of the fluorine content for the fluorinated SiN_x films. The binding energy of the Si $2p$ level increased monotonically from 102.15 to 102.70 eV which is corresponding to the increase in fluorine concentration in fluorinated SiN_x films, although the resolution of instrument (0.7 eV) is not sufficient to determine the precise peak position of binding energy. Therefore, we consider that Si–F bonds exist in the films. These facts indicate Si–H bonds have been replaced by Si–F bonds. The charge transfer from Si to the

Downloaded 19 Oct 2006 to 133.6.32.11. Redistribution subject to AIP license or copyright, see http://jap.aip.org/jap/copyright.jsp

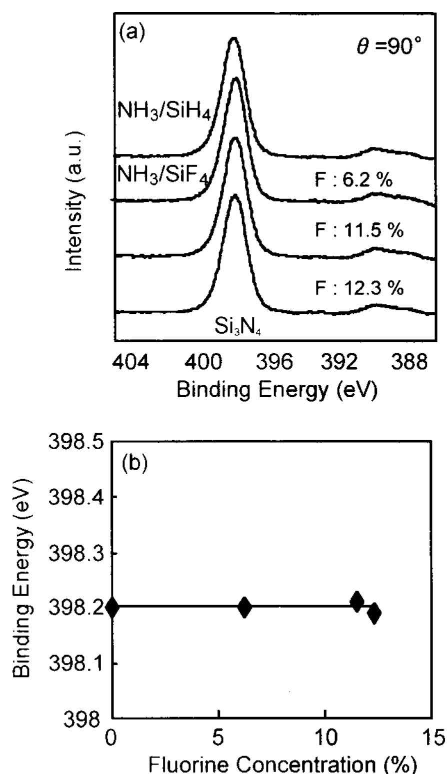

FIG. 4. (a) *In situ* XPS spectra of N 1*s* and (b) binding energy (relative to E_F) of N 1*s* core levels of SiN_x films as a function of fluorine concentration.

more electronegative F leaves a positive charge on the Si atom, which results in a shift of Si core levels towards higher binding energy.[11]

The N 1*s* spectra of conventional SiN_x film and fluorinated SiN_x films of various fluorine concentrations are shown in Fig. 4(a). Binding energies of the N 1*s* levels are plotted in Fig. 4(b) as a function of fluorine content for fluorinated SiN_x films. The binding energy shifts of the N 1*s* level are independent of the fluorine concentration, suggesting that Si–H_x bonds are replaced by Si–F_x bonds and that no N–F_x bonds exist in the fluorinated SiN_x films.

The chemical bonds of Si, N, F, and H in the SiN_x films were investigated by FTIR spectroscopy. Figure 5 shows the FTIR spectra of (a) SiN_x film formed employing NH_3/SiH_4

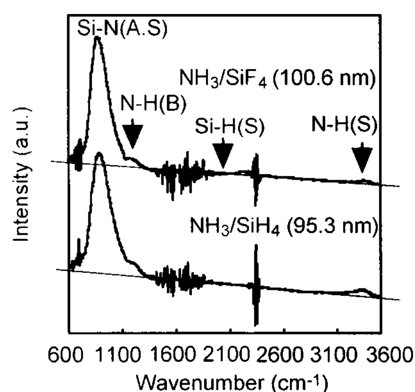

FIG. 5. FTIR spectra of (a) SiN_x film formed employing NH_3/SiH_4 and (b) fluorinated SiN_x film formed employing NH_3/SiF_4.

and (b) fluorinated SiN_x film formed employing NH_3/SiF_4 as well as the respective film thickness. In both cases, only the Si–N_x stretching mode ($820–870\ cm^{-1}$) and N–H stretching and bending mode (3340 and $1105\ cm^{-1}$) peaks are detected. Si–H stretching mode ($2050\ cm^{-1}$) signals were not observed. In the case of fluorinated SiN_x film, the large peak consists of Si–N_x peaks in terms of a superposition of Si–N_x and Si–F stretching mode ($940\ cm^{-1}$) components.[12,13] The hydrogen concentration of as-deposited fluorinated SiN_x film, as evaluated by the N–H stretching and bending modes, are reduced by less than 1/2 as compared to those of the SiN_x film formed employing NH_3/SiH_4. Tsu *et al.* reported that the SiN stretching mode frequency depends on the hydrogen concentration.[14] Since the frequency component of the SiN_x film consists of a superposition of Si–N stretching and N–H bending mode components, the Si–N stretching mode frequency depends on the amount of bonded hydrogen in N–H groups. The Si–N stretching mode frequency ($850.5\ cm^{-1}$) in the fluorinated SiN_x film was lower than that ($864\ cm^{-1}$) of the SiN_x film. These FTIR results indicate similar tendencies in the FTIR RAS results as shown in Fig. 1(a), which suggests that F atoms were scavenged by H atoms in the films. The addition of SiF_4 is thought to have occurred by H atoms being reduced by the kinetics of F atoms in the gas-phase reaction $F+H_2 \rightarrow HF+H$ and in the surface reaction $F+H \rightarrow HF$. These reactions reduce the Si–H and N–H bonds effectively in the fluorinated SiN_x films.

In order to investigate the stability of the films, TDS was performed. Figure 6 shows the TDS spectra of (a) SiN_x film formed employing NH_3/SiH_4 and (b) fluorinated SiN_x film formed employing NH_3/SiF_4. Several M/e (mass-to-charge ratio) fragments were detected from the fluorinated SiN_x films. The amount of desorption gas of $H_2(M/e=2)$ was observed to be above 350 °C. Notably, the amount of desorption gas of H_2 from the fluorinated SiN_x film was considerably lower than that of the SiN_x film, indicating that the hydrogen concentration in the fluorinated SiN_x film was much lower than that of the SiN_x film, which shows similar tendencies in the FTIR results. $M/e=19$ shows H_3O and/or F. However, the behaviors of intensities were stable and increased at 800 °C, which is identical for SiN_x and fluorinated SiN_x containing F atoms (11.5 at. %). The SiN_x film formed employing NH_3/SiH_4 has no F atoms, revealing the desorption of F atom to be negligible, even at the high temperature of 900 °C. Thus, F atoms in the fluorinated SiN_x film were very stable. As for desorption gas of $H(M/e=1)$ from the fluorinated SiN_x film, the behavior of these intensities were stable and increased at 700 °C, which is in good agreement with the behavior of the SiN_x film, suggesting that weak Si–H bonds (average bond energy: 3.18 eV) in the fluorinated film have been replaced by strong Si–F bonds (5.73 eV).[15]

In order to determine the energy band profile of the fluorinated SiN_x film, N 1*s* energy loss and valence band (VB) spectra were measured for the fluorinated SiN_x/Si(100) substrate using XPS as shown in Figs. 7(a) and 7(b).[16,17] The photoexcited electrons suffer inelastic losses due to plasmon and the band-to-band excitation. The plasmon loss signal exhibits a rather broad peak at 21–23 eV from the N 1*s* core

Downloaded 19 Oct 2006 to 133.6.32.11. Redistribution subject to AIP license or copyright, see http://jap.aip.org/jap/copyright.jsp

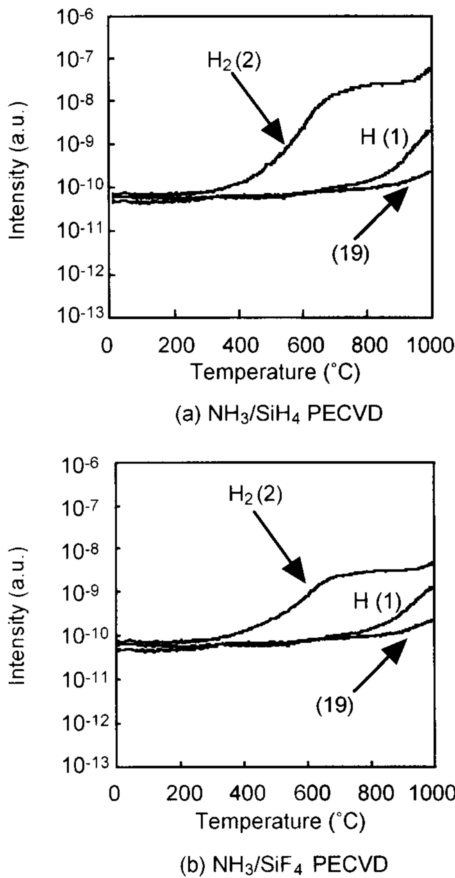

FIG. 6. TDS spectra of H, H_2, and F desorbed from (a) SiN_x film formed employing NH_3/SiH_4 and (b) fluorinated SiN_x film formed employing NH_3/SiF_4.

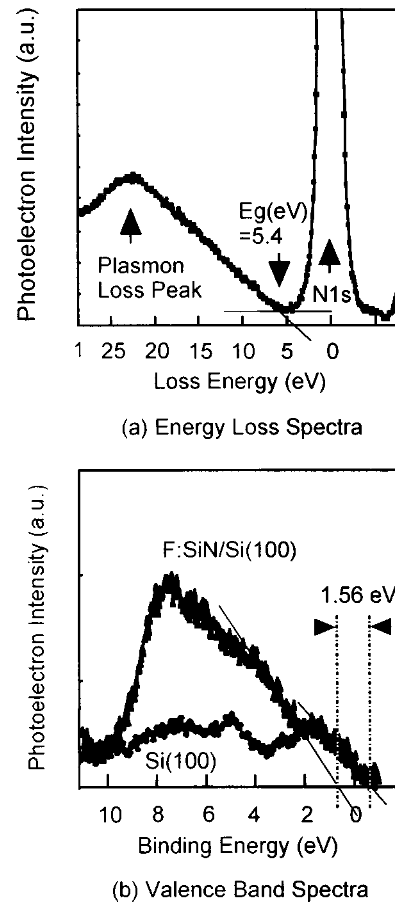

FIG. 7. (a) Energy loss spectra for fluorinated SiN_x film formed employing NH_3/SiF_4 and (b) valence band spectrum for the evaporated fluorinated SiN_x/Si(100) structure and the deconvoluted spectra for fluorinated SiN_x and Si(100).

level energy for fluorinated SiN_x film. The onset of the electron excitation from the valence to conduction band can also be observed at an energy separated by the band gap energy (E_g) from the core level peak as seen in Fig. 7(a). The E_g determined from the threshold energy of the energy loss spectrum was $5.4\,eV \pm 0.1\,eV$. Since the VB spectrum is composed of a mixture of the density of states (DOS) for fluorinated SiN_x film and Si(100) substrate, it can be deconvoluted using the valence band spectra separately measured for fluorinated SiN_x film and Si(100) substrate as indicated in Fig. 7(b). By subtracting the contribution of the Si(100) DOS measured for a hydrogen terminated Si(100) surface from the observed VB spectrum for the fluorinated SiN_x/Si(100) substrate, the VB alignment was obtained to be 1.56 eV. Using the measured VB offset and the E_g for the fluorinated SiN_x film and Si substrate, the conduction band barrier height at the fluorinated SiN_x/Si(100) substrate is estimated to be 2.72 eV. The barrier height obtained from XPS analysis is not an electrical property value but roughly estimated value. From these results, the energy band profile for the Al/fluorinated SiN_x/Si(100) structure in MNS devices can be determined as illustrated in Fig. 8. This results suggests that the leakage current in the MNS structure employing fluorinated SiN_x as a gate dielectric film can be suppressed considerably due to the electron barrier height being larger than 2 eV.

B. Electrical properties

Figure 9 shows leakage currents measured in SiN_x films that were formed employing NH_3/SiH_4, NH_3/SiF_4 and the conventional thermal SiO_2 films having an equivalent oxide thickness (EOT) of approximately 2.8 nm.[18] The leakage currents were found to be drastically decreased by employing NH_3/SiF_4. In particular, the $J-V$ characteristics exhibit the minimum leakage current in films formed by NH_3/SiF_4

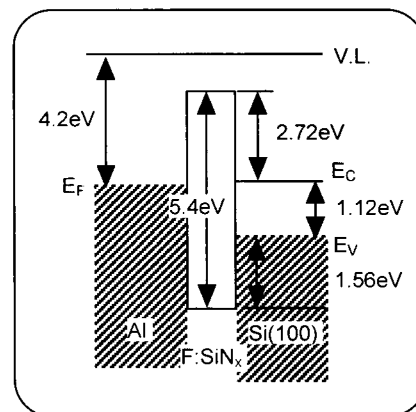

FIG. 8. Energy band profile for poly-Si/fluorinated SiN_x/Si(100) structure.

Downloaded 19 Oct 2006 to 133.6.32.11. Redistribution subject to AIP license or copyright, see http://jap.aip.org/jap/copyright.jsp

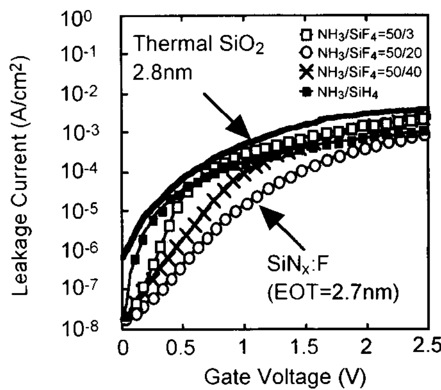

FIG. 9. $J-V$ characteristics for SiN_x films employing NH_3/SiH_4, NH_3/SiF_4 (50/3, 50/20, 50/40 sccm), and the conventional thermal SiO_2.

(50/20 sccm), of which concentration of F atom involved in the film is 11.5 at. %. The fluorinated SiN_x film formed by NH_3/SiF_4 reduced the leakage current by one order of magnitude below the that of the thermal SiO_2 of identical EOT. This beneficial effect of fluorinated SiN_x film on the leakage current has been attributed to stronger Si–F_x bonds that replace weaker Si–H_x bonds in the film.

Figure 10 shows typical $C-V$ curves for (a) SiN_x film formed employing NH_3/SiH_4 and (b) fluorinated SiN_x film formed employing NH_3/SiF_4, recorded at 0.1 MHz for which the series resistance effect was corrected. The gate voltage was swept from inversion to accumulation and back at a rate of 1250 mV/s. The hump and hysteresis (40 mV) attributed to charge traps in the SiN_x film were observed in the $C-V$ data of the SiN_x films that were formed employing NH_3/SiH_4: whereas, the hump was not observed in the $C-V$ data of the fluorinated SiN_x films that were formed employing NH_3/SiF_4, for which excellent hysteresis (20 mV) was achieved employing NH_3/SiF_4. These results suggest that the state trapping density of SiN_x films formed employing NH_3/SiF_4 is much lower than those formed employing NH_3/SiH_4, which would indicate that the F atom works effectively in replacing weaker bonds, i.e., Si dangling bonds and Si–H_x bonds. The dielectric constant of fluorinated SiN_x film was almost identical to that of the SiN_x film, the values of which were primarily dependent on the composition of the ratio of Si to N in the films. The N/Si ratio of the fluorinated SiN_x films was approximately 0.95 (Si rich), and the estimated dielectric constant was approximately 6. The minimum value of the interface trap density (D_{it}) was obtained from the $C-V$ characteristics by means of the equation[19]

$$C_{it}=qD_{it}=\left(\frac{1}{C_{LF}}-\frac{1}{C_1}\right)^{-1}-\left(\frac{1}{C_{HF}}-\frac{1}{C_1}\right)^{-1},$$

where C_{LF} and C_{HF} are the values of the capacitance of the MIS at low and high frequencies, respectively, and C_1 is the capacitance of the fluorinated SiN_x film. Thus, the minimum value of D_{it} was estimated to be $4\times10^{11}\,cm^{-2}$, which is the lower value described for the SiN_x/Si interface.[20] From these results, the ultrathin fluorinated SiN_x film appears extremely promising for application in gate dielectric film in next generation ULSIs.

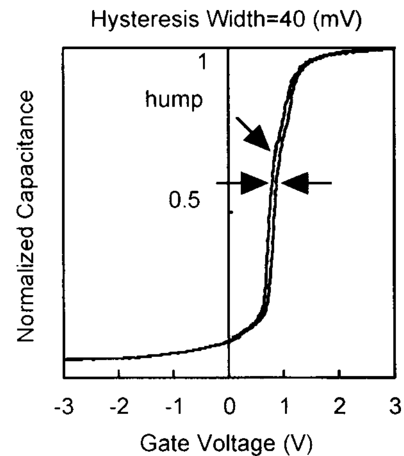

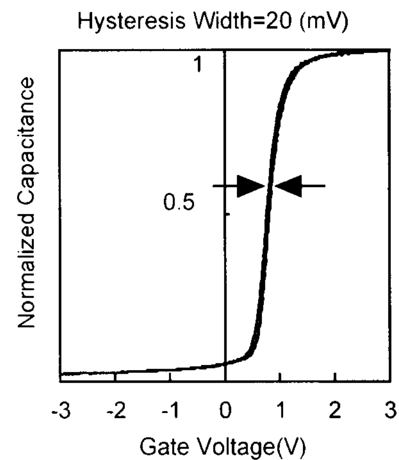

FIG. 10. Typical capacitance–voltage curves recorded at 0.1 MHz for (a) SiN_x film formed employing NH_3/SiH_4 and (b) fluorinated SiN_x film formed employing NH_3/SiF_4.

IV. CONCLUSIONS

We synthesized ultrathin fluorinated silicon nitride (SiN_x) films of 4 nm in thickness formed on a Si-substrate at 350 °C in ECR–PECVD employing NH_3/SiF_4 gases. The ultrathin fluorinated SiN_x film was evaluated as a gate dielectric film, and was found to have a low leakage current, reduced by several orders of magnitude compared to the thermal SiO_2 in the identical EOT, no hump, an excellent hysteresis loop (20 mV) and an interface trap density ($D_{it}=4\times10^{11}\,cm^{-2}$) in the $C-V$ characteristics. The film structures and the surface reactions for the fluorinated SiN_x film formation were discussed based on *in situ* XPS, *in situ* FTIR RAS, *in situ* AFM, and TDS observations. These *in situ* analyses indicated that the Si–H bonds in the film were replaced by F atoms without degrading the Si–N bonds, thus introducing optimum fluorine concentration into the film in PECVD via NH_3/SiF_4 plasma chemistry. The surface was smooth and the fluorine bonds in the fluorinated SiN_x film were found to be very stable and the amount of H atoms was very small as compared to PECVD employing NH_3/SiH_4. The control of fluorine concentration in the SiN_x films was

Downloaded 19 Oct 2006 to 133.6.32.11. Redistribution subject to AIP license or copyright, see http://jap.aip.org/jap/copyright.jsp

found to be a key factor in forming fluorinated SiN_x films of high quality at low temperatures. In addition, the energy band profile for Al/fluorinated SiN_x/Si(100) structure was determined. Consequently, the fluorinated SiN_x is thought to be a very effective material for use in ultrathin gate dielectric films in next generation ULSIs.

ACKNOWLEDGMENT

The authors would like to thank S. Fukuyama at Fujitsu Laboratory for performing the TDS measurements of the present study.

[1] D. Wang, T. Ma, J. W. Golz, B. L. Halpern, and J. J. Schmitt, IEEE Electron Device Lett. **13**, 482 (1992).
[2] T. Ohmi, S. Imai, and T. Hashimoto, IEICE (J72-C-11 542) (1989).
[3] D. G. Park *et al.*, J. Vac. Sci. Technol. B **14**, 2674 (1996).
[4] G. Lucovsky, P. D. Richard, D. V. Tsu, S. Y. Lin, and R. J. Markunas, J. Vac. Sci. Technol. A **4**, 681 (1986).
[5] K. Sekine, Y. Saito, M. Hirayama, and T. Ohmi, J. Vac. Sci. Technol. A **17**, 3129 (1999).
[6] H. Iwai, H. S. Momose, T. Morimoto, S. Takagi, and K. Yamabe, ESSDERC 1990, p. 287.
[7] H. Ohta, A. Nagashima, M. Ito, M. Hori, and T. Goto, J. Vac. Sci. Technol. B **18**, 2486 (2000).
[8] H. Ohta, A. Nagashima, M. Hori, and T. Goto, J. Appl. Phys. (in press).
[9] R. Nozawa, H. Takeda, M. Ito, M. Hori, and T. Goto, J. Appl. Phys. **81**, 8035 (1997).
[10] T. Wadayama and W. Suetake, Surf. Sci. **218**, L490 (1989).
[11] C. H. F. Peden, J. W. Rogers, Jr., N. D. Shinn, K. B. Kidd, and K. L. Tsang, Phys. Rev. B **47**, 15622 (1993).
[12] D. V. Tsu and G. Lucovsky, J. Vac. Sci. Technol. A **4**, 480 (1986).
[13] M. Ino, N. Inoue, and M. Yoshimaru, IEEE Trans. Electron Devices **41**, 703 (1998).
[14] D. V. Tsu, G. Lucovsky, and M. J. Mantini, Phys. Rev. B **33**, 7069 (1986).
[15] P. Chowdhury, A. I. Chou, K. Kumar, C. Lin, and J. C. Lee, Appl. Phys. Lett. **70**, 37 (1997).
[16] R. Karcher, L. Ley, and R. L. Johnson, Phys. Rev. B **30**, 1896 (1984).
[17] H. Itokawa, T. Maruyama, S. Miyazaki, and M. Hirose, Solid State Device and Materials, Tokyo, 1999, p. 158.
[18] T. P. Ma, IEEE Trans. Electron Devices **45**, 680 (1998).
[19] E. H. Nicollian and J. R. Brews, *MOS Physics and Technology* (Wiley, New York, 1982).
[20] S. Garcia *et al.*, J. Appl. Phys. **83**, 332 (1998).

Downloaded 19 Oct 2006 to 133.6.32.11. Redistribution subject to AIP license or copyright, see http://jap.aip.org/jap/copyright.jsp